Homogenization design method for biomorphic composite materials

Ronald H.W. Hoppe* and Svetozara I. Petrova**
Department of Mathematics, University of Augsburg, University Str. 14, D-86159 Augsburg, Germany

1. Introduction

Biomimetics is a multidisciplinary science that aims at the abstraction of design principles from nature by mimicking the structural composition and functionality of biological objects (cf., e.g., [1]). An important new technology in biomimetics is *biotemplating* which stands for the material synthesis of biologically grown materials into microcellular ceramic composites.

Biomorphic microcellular silicon carbide (SiC) ceramics with variable pore size, pore morphology, and strut thickness have been recently manufactured from natural grown plant materials like wood and various wood products (cf., e.g., [2,3] and the references therein). Experiments show that their anisotropic porous microstructures are one-to-one pseudomorphous to the original wood material. The microscopical morphology and the materials properties strongly depend on the used biotemplating technology: i) liquid Si-infiltration; ii) gaseous SiO-, Si-, and MTS (methyltrichlorosilane)- infiltration; iii) infiltration of Si-organic polymers (see Fig. 1 for infiltration of pine wood template).

The production of biomorphic SiC ceramics is done in two steps: a preprocessing step involving high-temperature pyrolysis (800–1800°C in inert atmosphere) and a subsequent infiltration of the resulting carbon preform by liquid or gaseous silicon at 1600°C which reacts with the carbon to result in a porous SiC ceramic material. A detailed description of the high-temperature synthesis can be found in [2,3].

*Corresponding author.
**Permanent address: Central Laboratory for Parallel Processing, Bulgarian Academy of Sciences, Acad. G. Bontchev Str., Block 25A, 1113 Sofia, Bulgaria.

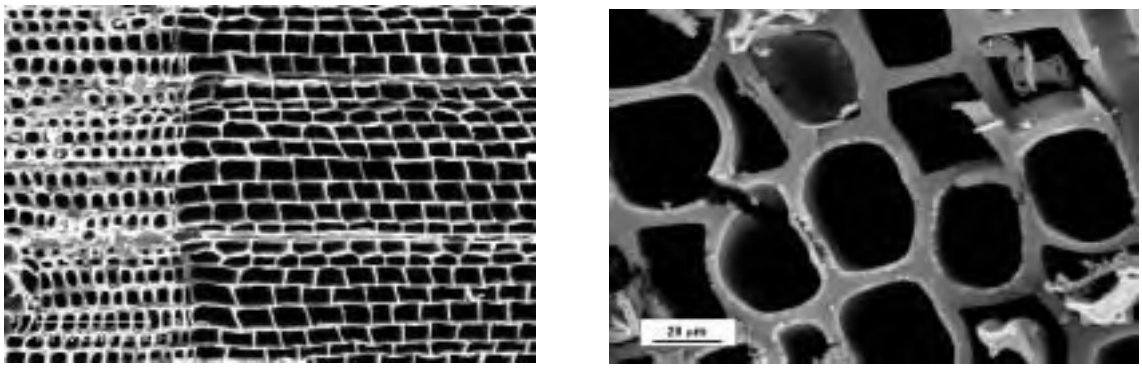

Fig. 1. SEM micrographs: a) Si-gas infiltration; b) Si-polymer infiltration.

Biological materials and organic fibres are available on a commercial scale, they are less expensive and naturally regenerating. Wood and organic fibres can be easily machined, preformed into complex 3-dimensional shapes of different porosity and cellular structure with a large variety in cell diameters ranging from micrometer (wood structures) up to the millimeter level (e.g., preprocessed papers). The large variety of natural plant morphologies facilitate the manufacturing of porous ceramic microstructures with a tailored microstructure and composition.

The optimal design of microstructured devices by homogenization modeling is by now a well established technique in structural mechanics (cf., e.g., [4–8]). Homogenization is performed to avoid a cost-prohibitive resolution of the microstructural details. Optimization methods are applied to the homogenized model and involve an iterative process where the numerical solution of the discretized state equation and the optimization routine are handled separately.

This paper is organized as follows. Section 2 deals with the optimal structural design of the ceramic composites by homogenization technique. Primal-dual interior-point method is proposed to solve the equality and inequality constrained nonconvex optimization problem. In contrast to traditional design strategies, this technique represents an all-in-one approach where the numerical solution of the state equation is an integral part of the optimization routine. Solution technique for the condensed primal-dual system is proposed in Section 3 by using transforming iterations as iterative procedure. The last section comments on the choice of merit functions and application of the line-search method to find successful increments for the unknown primal and dual variables.

2. Structural optimization by homogenization

For the optimal structural design a macroscopic scale model has been provided by the homogenization approach assuming periodically distributed quadratic microcells Y consisting of an interior part treated as a weak material surrounded by a layer of SiC and an outer layer of carbon (C). Assuming linear elasticity for the constituents of our composite material, the homogenized elasticity tensor $\mathbf{E}^H = \left(E^H_{ijkl}\right)$ is given (cf., e.g., [9,10]) by

$$E^H_{ijkl} = \frac{1}{|Y|}\int_Y \left(E_{ijkl}(y) - E_{ijpq}(y)\frac{\partial \xi^{kl}_p}{\partial y_q} \right) dy,$$

where $E_{ijkl}(y)$ are piecewise constant in Y and $\xi_p^{kl} \in H^1_{\text{per}}(Y)$ satisfies

$$\int_Y \left(E_{ijpq}(y) \frac{\partial \xi_p^{kl}}{\partial y_q} \right) \frac{\partial \phi_i}{\partial y_j} \, dy = \int_Y E_{ijkl}(y) \frac{\partial \phi_i}{\partial y_j} \, dy, \qquad \forall \boldsymbol{\phi} \in V_Y .$$

Here, V_Y is the set of all admissible Y-periodic virtual displacement fields.

Denote by $\boldsymbol{\mu} = (\mu_1, \mu_2)^T$ the vector of the lengths of the silicon carbide and carbon layers in the microstructure, and by θ the angle of cell rotation. Note that these variables serve as design parameters in our structural optimization. The dependence of the homogenized elasticity tensor on these quantities has been computed on the basis of a conforming P1 discretization. We consider further the rotated homogenized elasticity tensor

$$\mathbf{E}^R = \begin{pmatrix} E^R_{1111} & E^R_{1122} & E^R_{1112} \\ E^R_{2211} & E^R_{2222} & E^R_{2212} \\ E^R_{1211} & E^R_{1222} & E^R_{1212} \end{pmatrix},$$

where for the components R_{ij} of the rotated matrix we have

$$E^R_{ijkl} = \sum_{m,n,p,q=1}^{2} E^H_{mnpq}(\mu_1, \mu_2) \, R_{im}(\theta) \, R_{jn}(\theta) \, R_{kp}(\theta) \, R_{lq}(\theta), \;\; i,j,k,l = 1,2.$$

Furthermore, we compute the optimal distribution of our composite material in a given domain $\Omega \subset \mathcal{R}^2$ where a surface traction $\mathbf{t}$ is applied to a part of the boundary $\Gamma_T \subset \partial\Omega$ and known displacements $\mathbf{g}$ are specified on the remaining portion Γ_D ($\Gamma_D \cup \Gamma_T = \partial\Omega$). We assume a design composite with a square hole located at the center of the unit microcell Y.

As far as the structural optimization is concerned, we consider the mean compliance of the structure

$$J(\mathbf{u}, \alpha) = \int_\Omega \mathbf{f} \cdot \mathbf{u} \, dx + \int_{\Gamma_T} \mathbf{t} \cdot \mathbf{u} \, ds \tag{1}$$

as the objective functional where $\mathbf{f}$ is the external body force applied to Ω. The displacement vector $\mathbf{u} = (u_1, u_2)^T$ represents the *state variables* and the vector $\boldsymbol{\alpha} = (\mu_1, \mu_2, \theta)^T$ stands for the *design parameters*.

For a given constant M our optimization problem has the form

$$J(\mathbf{u}, \alpha) = \inf_{\mathbf{v}, \boldsymbol{\beta}} J(\mathbf{v}, \boldsymbol{\beta}),$$

subject to the following equality and inequality constraints

$$\sum_{i,j,k,l=1}^{2} \int_\Omega E^R_{ijkl}(x) \frac{\partial u_k}{\partial x_l} \frac{\partial \phi_i}{\partial x_j} \, dx = \int_\Omega \mathbf{f} \cdot \boldsymbol{\phi} \, dx + \int_{\Gamma_T} \mathbf{t} \cdot \boldsymbol{\phi} \, ds, \;\; \forall \boldsymbol{\phi} \in V_0 \tag{2}$$

$$g(\boldsymbol{\mu}) := \sum_{i=1}^{2} \mu_i = M \, , \qquad \mu_{\min} \mathbf{e} \le \boldsymbol{\mu} \le \mu_{\max} \mathbf{e}, \tag{3}$$

for constants $\mu_{\min} = 0,\ \mu_{\max} = 0.5$. Note that Eq. (2) is the weak form of the rotated homogenized equilibrium equation. Here, $\boldsymbol{u} \in V_D = \{\mathbf{v} \in \mathbf{H}^1(\Omega) | \mathbf{v} = \mathbf{g} \text{ on } \Gamma_D\}$ and $V_0 = \{\mathbf{v} \in \mathbf{H}^1(\Omega) | \mathbf{v} = \mathbf{0} \text{ on } \Gamma_D\}$.

The state variables are discretized by conforming P1 elements with respect to a simplicial triangulation of Ω whereas the design variables are approximated by elementwise constants. The discretized nonlinear constrained minimization problem has the following form

$$J(\boldsymbol{u}, \boldsymbol{\mu}, \theta) = \inf_{\boldsymbol{v}, \boldsymbol{\sigma}, \gamma} J(\boldsymbol{v}, \boldsymbol{\sigma}, \gamma), \tag{4}$$

subject to

$$\begin{aligned} A(\boldsymbol{\mu}, \theta)\, \boldsymbol{u} - \mathbf{b} = 0, \qquad & \boldsymbol{\mu} - \mu_{\min}\mathbf{e} \geqslant 0, \\ g(\boldsymbol{\mu}) - \mathrm{M} = 0, \qquad & \mu_{\max}\mathbf{e} - \boldsymbol{\mu} \geqslant 0, \end{aligned} \tag{5}$$

where $\mathbf{e} = (1,1)^T$, $A(\boldsymbol{\mu}, \theta)$ is the stiffness matrix corresponding to Eq. (2), $\mathbf{b}$ is the discrete load vector. Note that $\mu_i = 0,\ i = 1, 2$, corresponds to a complete void, $\mu_1 + \mu_2 = 0.5$ corresponds to a complete solid material, and $0 < \mu_1, \mu_2 < 0.5$ and $0 < \mu_1 + \mu_2 < 0.5$ to the porous composite with a void at a microlevel.

The discretized constrained minimization problem is solved by primal-dual interior-point method substituting the inequality constraints in Eq. (5) by logarithmic barrier functions. Assuming that $\boldsymbol{\mu} > \mu_{\min}\,\mathbf{e}$ and $\mu_{\max}\,\mathbf{e} > \boldsymbol{\mu}$ this substitution results in the following parametrized family of optimization subproblems

$$\tilde{J}(\boldsymbol{u}, \boldsymbol{\mu}, \theta) = \inf_{\boldsymbol{v}, \boldsymbol{\sigma}, \gamma} [J(\boldsymbol{v}, \boldsymbol{\sigma}, \gamma) - \rho\ (\log(\boldsymbol{\sigma} - \mu_{\min}\mathbf{e}) + \log(\mu_{\max}\mathbf{e} - \boldsymbol{\sigma}))] \tag{6}$$

subject to the equality constraints

$$A(\boldsymbol{\mu}, \theta)\, \boldsymbol{u} - \mathbf{b} = 0, \qquad g(\boldsymbol{\mu}) - \mathrm{M} = 0, \tag{7}$$

where $\rho > 0$ is a suitably chosen barrier parameter. Coupling the equality constraints by Lagrangian multipliers we have the following Lagrangian function associated with the problem Eqs (6) and (7)

$$\begin{aligned} L_\rho(\boldsymbol{u}, \boldsymbol{\mu}, \theta; \boldsymbol{\lambda}, \eta) := {} & J(\boldsymbol{u}, \boldsymbol{\mu}, \theta) - \rho\ (\log(\boldsymbol{\mu} - \mu_{\min}\,\mathbf{e}) + \log(\mu_{\max}\,\mathbf{e} - \boldsymbol{\mu})) \\ & + \boldsymbol{\lambda}^T (A(\boldsymbol{\mu}, \theta)\, \boldsymbol{u} - \mathbf{b}) + \eta\, (g(\boldsymbol{\mu}) - \mathrm{M}). \end{aligned}$$

The first-order Karush-Kuhn-Tucker (KKT) conditions are given by

$$\mathbf{F}^\rho(\boldsymbol{u}, \boldsymbol{\mu}, \theta; \boldsymbol{\lambda}, \eta) = \mathbf{0}\,, \tag{8}$$

where

$$\begin{aligned} F_1^\rho &= \nabla_{\boldsymbol{u}} L_\rho = \nabla_{\boldsymbol{u}}\, J + A(\boldsymbol{\mu}, \theta)^T \boldsymbol{\lambda}\,, \\ F_2^\rho &= \nabla_{\boldsymbol{\mu}} L_\rho = \partial_{\boldsymbol{\mu}}(\boldsymbol{\lambda}^T A(\boldsymbol{\mu}, \theta)\boldsymbol{u}) + \eta \nabla g(\boldsymbol{\mu}) - \rho D_1^{-1}\mathbf{e} + \rho D_2^{-1}\mathbf{e}\,, \\ F_3^\rho &= \nabla_\theta L_\rho = \partial_\theta(\boldsymbol{\lambda}^T A(\boldsymbol{\mu}, \theta)\boldsymbol{u})\,, \\ F_4^\rho &= \nabla_{\boldsymbol{\lambda}} L_\rho = A(\boldsymbol{\mu}, \theta)\, \boldsymbol{u} - \mathbf{b}\,, \\ F_5^\rho &= \nabla_\eta L_\rho = g(\boldsymbol{\mu}) - \mathrm{M}\,, \end{aligned} \tag{9}$$

and $D_1 := \mathrm{diag}(\mu_i - \mu_{\min})$ and $D_2 := \mathrm{diag}(\mu_{\max} - \mu_i)$, $i = 1, 2$. Since for $\rho \to 0$ the expressions $\rho D_1^{-1}\mathbf{e}$ and $\rho D_2^{-1}\mathbf{e}$ approximate the complementarity conditions associated with Eq. (5) it is standard to introduce $\boldsymbol{z} := \rho D_1^{-1}\mathbf{e} \geqslant \mathbf{0}$ and $\boldsymbol{w} := \rho D_2^{-1} \geqslant \mathbf{0}$ serving as *perturbed complementarity*. Then, the primal-dual Newton-type interior-point method is applied to three sets of variables: primal feasibility $(\boldsymbol{u}, \boldsymbol{\mu}, \theta)$, dual feasibility $(\boldsymbol{\lambda}, \eta)$, and perturbed complementarity related to $(\boldsymbol{z}, \boldsymbol{w})$.

Denote the Lagrangian function of problem Eqs (4) and (5) by

$$\begin{aligned} L(\boldsymbol{u}, \boldsymbol{\mu}, \theta; \boldsymbol{\lambda}, \eta; \boldsymbol{z}, \boldsymbol{w}) := J(\boldsymbol{u}, \boldsymbol{\mu}, \theta) \\ + \boldsymbol{\lambda}^T (A(\boldsymbol{\mu}, \theta)\, \boldsymbol{u} - \mathbf{b}) + \eta\, (g(\boldsymbol{\mu}) - \mathrm{M}) \\ - \boldsymbol{z}^T (\boldsymbol{\mu} - \mu_{\min}\, \mathbf{e}) - \boldsymbol{w}^T (\mu_{\max}\, \mathbf{e} - \boldsymbol{\mu}). \end{aligned} \tag{10}$$

The Newton method applied to the KKT conditions of Eq. (10) results in

$$\begin{pmatrix} 0 & L_{\boldsymbol{u}\boldsymbol{\mu}} & L_{\boldsymbol{u}\theta} & L_{\boldsymbol{u}\boldsymbol{\lambda}} & 0 & 0 & 0 \\ L_{\boldsymbol{\mu}\boldsymbol{u}} & L_{\boldsymbol{\mu}\boldsymbol{\mu}} & L_{\boldsymbol{\mu}\theta} & L_{\boldsymbol{\mu}\boldsymbol{\lambda}} & L_{\boldsymbol{\mu}\eta} & -\mathrm{I} & \mathrm{I} \\ L_{\theta\boldsymbol{u}} & L_{\theta\boldsymbol{\mu}} & L_{\theta\theta} & L_{\theta\boldsymbol{\lambda}} & 0 & 0 & 0 \\ L_{\boldsymbol{\lambda}\boldsymbol{u}} & L_{\boldsymbol{\lambda}\boldsymbol{\mu}} & L_{\boldsymbol{\lambda}\theta} & 0 & 0 & 0 & 0 \\ 0 & L_{\eta\boldsymbol{\mu}} & 0 & 0 & 0 & 0 & 0 \\ 0 & Z & 0 & 0 & 0 & D_1 & 0 \\ 0 & -W & 0 & 0 & 0 & 0 & D_2 \end{pmatrix} \begin{pmatrix} \triangle \boldsymbol{u} \\ \triangle \boldsymbol{\mu} \\ \triangle \theta \\ \triangle \boldsymbol{\lambda} \\ \triangle \eta \\ \triangle \mathbf{z} \\ \triangle \mathbf{w} \end{pmatrix} = - \begin{pmatrix} \nabla_{\boldsymbol{u}} L \\ \nabla_{\boldsymbol{\mu}} L \\ \nabla_{\theta} L \\ \nabla_{\boldsymbol{\lambda}} L \\ \nabla_{\eta} L \\ \nabla_{\boldsymbol{z}} L \\ \nabla_{\boldsymbol{w}} L \end{pmatrix}, \tag{11}$$

where I stands for the identity matrix, $Z = \mathrm{diag}(z_i)$ and $W = \mathrm{diag}(w_i)$, $i = 1, 2$, are diagonal matrices. The coefficient matrix Eq. (11) is usually referred to as the *primal-dual system*. It can be easily symmetrized since the matrices Z and W are diagonal. We do not use this approach here but instead perform a block elimination of the increments $\triangle \mathbf{z}$ and $\triangle \mathbf{w}$ yielding the *condensed primal-dual system*

$$\begin{pmatrix} 0 & L_{\boldsymbol{u}\boldsymbol{\mu}} & L_{\boldsymbol{u}\theta} & L_{\boldsymbol{u}\boldsymbol{\lambda}} & 0 \\ L_{\boldsymbol{\mu}\boldsymbol{u}} & \tilde{L}_{\boldsymbol{\mu}\boldsymbol{\mu}} & L_{\boldsymbol{\mu}\theta} & L_{\boldsymbol{\mu}\boldsymbol{\lambda}} & L_{\boldsymbol{\mu}\eta} \\ L_{\theta\boldsymbol{u}} & L_{\theta\boldsymbol{\mu}} & L_{\theta\theta} & L_{\theta\boldsymbol{\lambda}} & 0 \\ L_{\boldsymbol{\lambda}\boldsymbol{u}} & L_{\boldsymbol{\lambda}\boldsymbol{\mu}} & L_{\boldsymbol{\lambda}\theta} & 0 & 0 \\ 0 & L_{\eta\boldsymbol{\mu}} & 0 & 0 & 0 \end{pmatrix} \begin{pmatrix} \triangle \boldsymbol{u} \\ \triangle \boldsymbol{\mu} \\ \triangle \theta \\ \triangle \boldsymbol{\lambda} \\ \triangle \eta \end{pmatrix} = - \begin{pmatrix} \nabla_{\boldsymbol{u}} L \\ \tilde{\nabla}_{\boldsymbol{\mu}} L \\ \nabla_{\theta} L \\ \nabla_{\boldsymbol{\lambda}} L \\ \nabla_{\eta} L \end{pmatrix}, \tag{12}$$

where

$$\tilde{L}_{\boldsymbol{\mu}\boldsymbol{\mu}} := L_{\boldsymbol{\mu}\boldsymbol{\mu}} + D_1^{-1} Z + D_2^{-1} W$$

and the modified entry for the right-hand side is

$$\tilde{\nabla}_{\boldsymbol{\mu}} L := \nabla_{\boldsymbol{\mu}} L + D_1^{-1} \nabla_{\mathbf{z}} L - D_2^{-1} \nabla_{\mathbf{w}} L.$$

In the case of structural optimization of electromagnetic devices some details of solving the condensed primal-dual system by primal-dual interior-point method using damped Newton iterations can be found in [11].

3. Solution technique

In this section, we consider the *null space* decomposition of the condensed primal-dual system Eq. (12) interchanging the second and the forth rows and columns. The resulting matrix can be written according to

$$K = \begin{pmatrix} A & B^T \\ B & D \end{pmatrix} = \left(\begin{array}{cc|ccc} 0 & L_{\boldsymbol{u\lambda}} & L_{\boldsymbol{u\mu}} & L_{\boldsymbol{u}\theta} & 0 \\ L_{\boldsymbol{\lambda u}} & 0 & L_{\boldsymbol{\lambda\mu}} & L_{\boldsymbol{\lambda}\theta} & 0 \\ \hline L_{\boldsymbol{\mu u}} & L_{\boldsymbol{\mu\lambda}} & \tilde{L}_{\boldsymbol{\mu\mu}} & L_{\boldsymbol{\mu}\theta} & L_{\boldsymbol{\mu}\eta} \\ L_{\theta\boldsymbol{u}} & L_{\theta\boldsymbol{\lambda}} & L_{\theta\boldsymbol{\mu}} & L_{\theta\theta} & 0 \\ 0 & 0 & L_{\eta\boldsymbol{\mu}} & 0 & 0 \end{array}\right), \tag{13}$$

where the first diagonal block

$$A = \begin{pmatrix} 0 & L_{\boldsymbol{u\lambda}} \\ L_{\boldsymbol{\lambda u}} & 0 \end{pmatrix} \tag{14}$$

is now an indefinite, but nonsingular matrix. We remind that $L_{\boldsymbol{\lambda u}} = A(\boldsymbol{\mu}, \theta)$ is exactly the stiffness matrix corresponding to the rotated homogenized state equation. Hence, A^{-1} exists, and the Schur complement $S := D - BA^{-1}B^T$ is correctly defined.

We use now the following regular splitting of K

$$K^L K K^R = M_1 - M_2 \tag{15}$$

with left and right factors given below and reasonable matrices M_1 and $M_2 \sim 0$. For solving system of the form $K\triangle\boldsymbol{\psi} = \boldsymbol{\xi}$, starting with an initial guess for $\triangle\boldsymbol{\psi} := (\triangle\boldsymbol{u}, \triangle\boldsymbol{\lambda}, \triangle\boldsymbol{\mu}, \triangle\theta, \triangle\eta)^T$, the transforming iteration proposed in [12] is described by

$$\triangle\boldsymbol{\psi}^{\nu+1} := \triangle\boldsymbol{\psi}^{\nu} + K^R M_1^{-1} K^L(\boldsymbol{\xi} - K\triangle\boldsymbol{\psi}^{\nu}), \tag{16}$$

where the new iterate $\boldsymbol{\psi}^{\text{new}}$ is obtained by a line-search in the direction $\triangle\boldsymbol{\psi}$, namely

$$\psi_i^{\text{new}} = \psi_i^{\text{old}} + s_i(\triangle\psi)_i, \qquad 1 \le i \le 5.$$

The line-search approach and the choice of the steplengths parameters s_i is discussed in detail in Section 4.

Using an appropriate preconditioner for the stiffness matrix we approximate the first diagonal block Eq. (14) as follows

$$A = \begin{pmatrix} 0 & L_{\boldsymbol{u\lambda}} \\ L_{\boldsymbol{\lambda u}} & 0 \end{pmatrix} \sim \begin{pmatrix} 0 & \tilde{L}_{\boldsymbol{u\lambda}} \\ \tilde{L}_{\boldsymbol{\lambda u}} & 0 \end{pmatrix} =: \tilde{A}. \tag{17}$$

Usually applied left and right transformations are of the form

$$K^L = I, \qquad K^R = \begin{pmatrix} I & -\tilde{A}^{-1}B^T \\ 0 & I \end{pmatrix} = \left(\begin{array}{cc|ccc} \mathrm{I} & 0 & -\tilde{L}_{\boldsymbol{\lambda u}}^{-1} L_{\boldsymbol{\lambda\mu}} & -\tilde{L}_{\boldsymbol{\lambda u}}^{-1} L_{\boldsymbol{\lambda}\theta} & 0 \\ 0 & \mathrm{I} & -\tilde{L}_{\boldsymbol{u\lambda}}^{-1} L_{\boldsymbol{u\mu}} & -\tilde{L}_{\boldsymbol{u\lambda}}^{-1} L_{\boldsymbol{u}\theta} & 0 \\ \hline 0 & 0 & \mathrm{I} & 0 & 0 \\ 0 & 0 & 0 & \mathrm{I} & 0 \\ 0 & 0 & 0 & 0 & \mathrm{I} \end{array}\right).$$

In this case, the regular splitting Eq. (15) becomes $KK^R = M_1 - M_2$ where

$$M_1 = \left(\begin{array}{cc|ccc} 0 & L_{\boldsymbol{u\lambda}} & 0 & 0 & 0 \\ L_{\boldsymbol{\lambda u}} & 0 & 0 & 0 & 0 \\ \hline L_{\boldsymbol{\mu u}} & L_{\boldsymbol{\mu\lambda}} & S_1 & S_3 & L_{\boldsymbol{\mu}\eta} \\ L_{\theta\boldsymbol{u}} & L_{\theta\boldsymbol{\lambda}} & S_4 & S_2 & 0 \\ 0 & 0 & L_{\eta\boldsymbol{\mu}} & 0 & 0 \end{array}\right) = \begin{pmatrix} A & 0 \\ R & Q \end{pmatrix} \tag{18}$$

and $M_2 \sim 0$ if we have a good preconditioner for the stiffness matrix. In our numerical experiments we choose a Cholesky decomposition of $L_{\boldsymbol{u\lambda}}$.

The second diagonal block Q in Eq. (18) is symmetric and indefinite given by

$$Q = \begin{pmatrix} S_1 & S_3 & L_{\boldsymbol{\mu}\eta} \\ S_4 & S_2 & 0 \\ L_{\eta\,\boldsymbol{\mu}} & 0 & 0 \end{pmatrix},$$

where S_1 and S_2 defined below are symmetric matrices and $S_3 = S_4^T$, namely

$$\begin{aligned} S_1 &= \tilde{L}_{\boldsymbol{\mu\mu}} - L_{\boldsymbol{\mu u}}\tilde{L}^{-1}_{\boldsymbol{u\lambda}}L_{\boldsymbol{\lambda\mu}} - L_{\boldsymbol{\mu\lambda}}\tilde{L}^{-1}_{\boldsymbol{\lambda u}}L_{\boldsymbol{u\mu}}, \\ S_2 &= L_{\theta\theta} - L_{\theta\boldsymbol{u}}\tilde{L}^{-1}_{\boldsymbol{u\lambda}}L_{\boldsymbol{\lambda}\,\theta} - L_{\theta\boldsymbol{\lambda}}\tilde{L}^{-1}_{\boldsymbol{\lambda u}}L_{\boldsymbol{u}\,\theta}, \\ S_3 &= L_{\boldsymbol{\mu}\theta} - L_{\boldsymbol{\mu u}}\tilde{L}^{-1}_{\boldsymbol{u\lambda}}L_{\boldsymbol{\lambda}\,\theta} - L_{\boldsymbol{\mu\lambda}}\tilde{L}^{-1}_{\boldsymbol{\lambda u}}L_{\boldsymbol{u}\,\theta}, \\ S_4 &= L_{\theta\boldsymbol{\mu}} - L_{\theta\boldsymbol{u}}\tilde{L}^{-1}_{\boldsymbol{u\lambda}}L_{\boldsymbol{\lambda\mu}} - L_{\theta\boldsymbol{\lambda}}\tilde{L}^{-1}_{\boldsymbol{\lambda u}}L_{\boldsymbol{u\mu}}. \end{aligned}$$

We denote the defect in Eq. (16) by $\boldsymbol{d} = \boldsymbol{\xi} - K\triangle\boldsymbol{\psi}^{\nu}$ and compute the corresponding entries

$$\begin{aligned} d_{\boldsymbol{u}} &= -\nabla_{\boldsymbol{u}}L - L_{\boldsymbol{u\lambda}}\triangle\boldsymbol{\lambda} - L_{\boldsymbol{u\mu}}\triangle\boldsymbol{\mu} - L_{\boldsymbol{u}\,\theta}\triangle\theta, \\ d_{\boldsymbol{\lambda}} &= -\nabla_{\boldsymbol{\lambda}}L - L_{\boldsymbol{\lambda u}}\triangle\boldsymbol{u} - L_{\boldsymbol{\lambda\mu}}\triangle\boldsymbol{\mu} - L_{\boldsymbol{\lambda}\theta}\triangle\theta, \\ d_{\boldsymbol{\mu}} &= -\tilde{\nabla}_{\boldsymbol{\mu}}L - L_{\boldsymbol{\mu u}}\triangle\boldsymbol{u} - L_{\boldsymbol{\mu\lambda}}\triangle\boldsymbol{\lambda} - \tilde{L}_{\boldsymbol{\mu\mu}}\triangle\boldsymbol{\mu} - L_{\boldsymbol{\mu}\theta}\triangle\theta - L_{\boldsymbol{\mu}\eta}\triangle\eta, \\ d_{\theta} &= -\nabla_{\theta}L - L_{\theta\boldsymbol{u}}\triangle\boldsymbol{u} - L_{\theta\boldsymbol{\lambda}}\triangle\boldsymbol{\lambda} - L_{\theta\boldsymbol{\mu}}\triangle\boldsymbol{\mu} - L_{\theta\theta}\triangle\theta, \\ d_{\eta} &= -\nabla_{\eta}L - L_{\eta\boldsymbol{\mu}}\triangle\boldsymbol{\mu}. \end{aligned}$$

Taking into account Eq. (16) one needs to compute

$$\boldsymbol{\delta} = M_1^{-1}\boldsymbol{d}, \text{ i.e., } M_1\boldsymbol{\delta} = \boldsymbol{d}.$$

Consequently, we find $\delta_{\boldsymbol{\lambda}} = \tilde{L}^{-1}_{\boldsymbol{u\lambda}}d_{\boldsymbol{u}}$ and $\delta_{\boldsymbol{u}} = \tilde{L}^{-1}_{\boldsymbol{\lambda u}}d_{\boldsymbol{\lambda}}$. To compute the remaining components of $\boldsymbol{\delta}$ we have to solve systems of the form $Q\boldsymbol{x} = \mathbf{f}$ with the indefinite matrix Q where

$$\mathbf{f} = (d_{\boldsymbol{\mu}} - L_{\boldsymbol{\mu u}}\delta_{\boldsymbol{u}} - L_{\boldsymbol{\mu\lambda}}\delta_{\boldsymbol{\lambda}},\, d_{\theta} - L_{\theta\boldsymbol{u}}\delta_{\boldsymbol{u}} - L_{\theta\boldsymbol{\lambda}}\delta_{\boldsymbol{\lambda}},\, d_{\eta})^T.$$

Iterative procedures as MINRES or Bi-CGSTAB (see [13]) with appropriate stopping criteria can be applied in this case.

MINRES method without preconditioning:

$k = 0$; Compute $\mathbf{r}_0 = \mathbf{f} - Q\,\mathbf{x}_0$ for some initial guess $\mathbf{x}_0$; $\mathbf{g}_0 = Q\,\mathbf{r}_0$;

while ($\|\mathbf{r}_k\|$ accurate enough)
  if $(k > 0)$ $\mathbf{g}_k = Q\,\mathbf{r}_k$;
  $\alpha = \mathbf{r}_k^T\,\mathbf{g}_k / \mathbf{g}_k^T\,\mathbf{g}_k$; $\mathbf{x}_{k+1} = \mathbf{x}_k + \alpha\,\mathbf{r}_k$; $\mathbf{r}_{k+1} = \mathbf{r}_k - \alpha\,\mathbf{g}_k$;
  check convergence; continue if necessary;
  $\mathbf{y} = Q\,\mathbf{g}_k$; $\beta = \mathbf{g}_k^T\,\mathbf{y} / \mathbf{g}_k^T\,\mathbf{g}_k$;
  if $(k = 0)$ $\gamma = 0$;
  else $\gamma = \mathbf{g}_{k-1}^T\,\mathbf{y} / \mathbf{g}_{k-1}^T\,\mathbf{g}_{k-1}$;
  endif;
  if $(k = 0)$ $\mathbf{r}_{k+1} = \mathbf{g}_k - \beta\,\mathbf{r}_k$; $\mathbf{g}_{k+1} = \mathbf{y} - \beta\,\mathbf{g}_k$;
  else $\mathbf{r}_{k+1} = \mathbf{g}_k - \beta\,\mathbf{r}_k - \gamma\,\mathbf{r}_{k-1}$; $\mathbf{g}_{k+1} = \mathbf{y} - \beta\,\mathbf{g}_k - \gamma\,\mathbf{g}_{k-1}$;
  endif;
  $\mathbf{g}_{k-1} = \mathbf{g}_k$, $\mathbf{g}_k = \mathbf{g}_{k+1}$; $\mathbf{r}_{k-1} = \mathbf{r}_k$, $\mathbf{r}_k = \mathbf{r}_{k+1}$;
  $k = k + 1$;

end;

Bi-CGSTAB method without preconditioning:

Select starting vector $\boldsymbol{x}_0 \in \mathcal{R}^n$, $\tilde{\boldsymbol{r}}_0 \in \mathcal{R}^n$

$\boldsymbol{r}_0 = \mathbf{f} - Q\boldsymbol{x}_0$; $\rho_0 = \alpha = \omega_0 := 1$;

$\boldsymbol{v}_0 = \boldsymbol{p}_0 = 0$;

For k = 1,2,3, ...
  $\rho_k = \tilde{\boldsymbol{r}}_0^T \boldsymbol{r}_{k-1}$; $\beta = (\rho_k/\rho_{k-1})(\alpha/\omega_{k-1})$
  $\boldsymbol{p}_k = \boldsymbol{r}_{k-1} + \beta(\boldsymbol{p}_{k-1} - \omega_{k-1}\boldsymbol{v}_{k-1})$;
  $\boldsymbol{v}_k = Q\boldsymbol{p}_k$;
  $\alpha = \rho_k / \tilde{\boldsymbol{r}}_0^T \boldsymbol{v}_k$;
  $\boldsymbol{s} = \boldsymbol{r}_{k-1} - \alpha\boldsymbol{v}_k$;
  $\boldsymbol{t} = Q\boldsymbol{s}$;
  $\omega_k = \boldsymbol{t}^T\boldsymbol{s} / \boldsymbol{t}^T\boldsymbol{t}$;
  $\boldsymbol{x}_k = \boldsymbol{x}_{k-1} + \alpha\boldsymbol{p}_k + \omega_k\boldsymbol{s}$;
  if $\boldsymbol{x}_k$ is accurate enough then quit;
  $\boldsymbol{r}_k = \boldsymbol{s} - \omega_k\boldsymbol{t}$.

4. Merit functions and line-search approach

For simplicity we denote in this section the primal variables by $\boldsymbol{x} = (\boldsymbol{u}, \boldsymbol{\mu}, \theta)$, the dual variables by $\boldsymbol{y} = (\boldsymbol{\lambda}, \eta)$, and the complementarity variables by $\boldsymbol{v} = (\boldsymbol{z}, \boldsymbol{w})$. A standard approach to choose a merit function for convergence is the l_2-norm $\|\mathbf{F}^\rho(\boldsymbol{u}, \boldsymbol{\mu}, \theta; \boldsymbol{\lambda}, \eta)\|$ of the residual resulting from the KKT conditions Eq. (8). A more realiable approach (cf., e.g. [11,14]) is to use two merit functions. Our

primary merit function is based on the logarithmic barrier function and the augmented Lagrangian term concerning only the equality constraints

$$M := M(\boldsymbol{x}, \boldsymbol{y}, \rho, \rho_A) = J(\boldsymbol{x}) - \rho \sum_{i=1}^{2} \log d_i(\boldsymbol{x}) + \boldsymbol{y}^T \boldsymbol{c}(\boldsymbol{x}) + \frac{1}{2}\rho_A \, \boldsymbol{c}(\boldsymbol{x})^T \boldsymbol{c}(\boldsymbol{x}), \tag{19}$$

where $\boldsymbol{c}(\boldsymbol{x}) = (c_1(\boldsymbol{x}), c_2(\boldsymbol{x}))$ and

$$\begin{aligned} c_1(\mathbf{x}) = c_1(\boldsymbol{u}, \boldsymbol{\mu}, \theta) = A(\boldsymbol{\mu}, \theta)\boldsymbol{u} - \mathbf{b},\ d_1(\mathbf{x}) = d_1(\boldsymbol{\mu}) = \boldsymbol{\mu} - \mu_{\min}\mathbf{e}, \\ c_2(\mathbf{x}) = c_2(\boldsymbol{\mu}) = g(\boldsymbol{\mu}) - \mathrm{M},\ d_2(\mathbf{x}) = d_2(\boldsymbol{\mu}) = \mu_{\max}\mathbf{e} - \boldsymbol{\mu}. \end{aligned} \tag{20}$$

The parameter ρ_A is a positive scalar which can be changed during the iteration in the case when $\triangle \boldsymbol{x} = (\triangle \boldsymbol{u}, \triangle \boldsymbol{\mu}, \triangle \theta)^T$ is not a descent direction for the primary merit function, i.e., $\triangle \boldsymbol{x}^T \nabla_{\boldsymbol{x}} M < 0$. The gradient of M with respect to $\boldsymbol{x}$ is

$$\nabla_{\boldsymbol{x}} M := \nabla_{\boldsymbol{x}} M(\boldsymbol{x}, \boldsymbol{y}, \rho, \rho_A) = \nabla J(\boldsymbol{x}) - \rho J_{\text{in}}^T D^{-1} \boldsymbol{e} + J_{\text{eq}}^T \boldsymbol{y} + \rho_A J_{\text{eq}}^T \boldsymbol{c}(\boldsymbol{x}), \tag{21}$$

where

$$J_{\text{eq}} = \begin{pmatrix} L_{\boldsymbol{\lambda u}} & L_{\boldsymbol{\lambda \mu}} & L_{\boldsymbol{\lambda}\theta} \\ 0 & L_{\eta \boldsymbol{\mu}} & 0 \end{pmatrix} \text{ and } J_{\text{in}} = \begin{pmatrix} 0 & \mathrm{I} & 0 \\ 0 & -\mathrm{I} & 0 \end{pmatrix}$$

with J_{eq} and J_{in} the Jacobian matrices corresponding to the equality and inequality constraints, respectively. Then we have

$$\begin{aligned} \triangle \boldsymbol{x}^T \nabla_{\boldsymbol{x}} M &= \triangle \boldsymbol{x}^T (\nabla J - \rho J_{\text{in}}^T D^{-1} \boldsymbol{e}) + \triangle \boldsymbol{x}^T J_{\text{eq}}^T \boldsymbol{y} + \rho_A \triangle \boldsymbol{x}^T J_{\text{eq}}^T \boldsymbol{c}(\boldsymbol{x}) \\ &= \triangle \boldsymbol{x}^T (\nabla J - \rho J_{\text{in}}^T D^{-1} \boldsymbol{e}) - \boldsymbol{c}(\boldsymbol{x})^T \boldsymbol{y} - \rho_A \boldsymbol{c}(\boldsymbol{x})^T \boldsymbol{c}(\boldsymbol{x}), \end{aligned} \tag{22}$$

taking into account that $J_{\text{eq}} \triangle \boldsymbol{x} = -c(\boldsymbol{x})$ according to the forth and fifth rows of the system Eq. (11). One can see from Eq. (22) that $\triangle \boldsymbol{x}^T \nabla_{\boldsymbol{x}} M < 0$ if

$$\rho_A > \frac{\triangle \boldsymbol{x}^T (\nabla J - \rho J_{\text{in}}^T D^{-1} \boldsymbol{e}) - c(\boldsymbol{x})^T \boldsymbol{y}}{c(\boldsymbol{x})^T c(\boldsymbol{x})}.$$

However, when $\triangle \boldsymbol{x}^T \nabla_{\boldsymbol{x}} M \geqslant 0$, ρ_A could achieve extreme large values for $\|\boldsymbol{c}\|$ being small. In this case, the following choice of ρ_A has been proposed (see, e.g., [14,11])

$$\rho_A = \min\left(\frac{5}{\boldsymbol{c}^T \boldsymbol{c}} \left(\triangle \boldsymbol{x}^T (\nabla J - \rho J_{\text{in}}^T D^{-1} \boldsymbol{e}) - \boldsymbol{c}(\boldsymbol{x})^T \boldsymbol{y} \right), 100 \right). \tag{23}$$

Our *secondary merit function* used for the line-search method is $\|\mathbf{F}^{\rho}(\boldsymbol{u}, \boldsymbol{\mu}, \theta; \boldsymbol{\lambda}, \eta)\|$. We consider only two parameters α and γ serving as steplengths for the primal variables and the complementarity conditions. Let $\hat{\alpha}_{\boldsymbol{\mu}}$, $\hat{\gamma}_{\mathbf{z}}$, and $\hat{\gamma}_{\mathbf{w}}$ be defined as

$$\begin{aligned} \hat{\alpha}_{\boldsymbol{\mu}} &= \max\left\{ \alpha \,|\, \mu_{\min}\mathbf{e} \leqslant \boldsymbol{\mu} + \alpha \triangle \boldsymbol{\mu} \leqslant \mu_{\max}\mathbf{e} \right\}, \\ \hat{\gamma}_{\mathbf{z}} &= \max\left\{ \gamma \,|\, \mathbf{z} + \gamma \triangle \mathbf{z} \geqslant 0 \right\}, \\ \hat{\gamma}_{\mathbf{w}} &= \max\left\{ \gamma \,|\, \mathbf{w} + \gamma \triangle \mathbf{w} \geqslant 0 \right\}. \end{aligned} \tag{24}$$

To ensure a strict feasibility, we define $\hat{\alpha} = \hat{\alpha}_{\boldsymbol{\mu}}$ and $\hat{\gamma} = \min(\hat{\gamma}_{\boldsymbol{z}}, \hat{\gamma}_{\boldsymbol{w}})$ and choose a positive parameter $\tau < 1$. The following steplengths then have been used

$$\alpha = \min(1, \tau\hat{\alpha}) \text{ and } \gamma = \min(1, \tau\hat{\gamma}).$$

Acknowledgements

This work has been partially supported by the German National Science Foundation (DFG) under Grant No.HO877/5-2. The second author has also been supported in part by the Bulgarian Ministry for Education and Science under Grant I1001/2000.

References

[1] M. Elices, ed., *Structural Biomaterials*, Princeton University Press, Princeton, 2000.
[2] P. Greil, T. Lifka and A. Kaindl, Biomorphic cellular silicon carbide ceramics from wood: I. Processing and microstructure, and II. Mechanical properties, *J. Europ. Ceramic Soc.* **18** (1998), 1961–1973 and 1975–1983,
[3] H. Sieber, C. Hoffmann, A. Kaindl and P. Greil, Biomorphic cellular ceramics, *Advanced Engineering Materials* **2** (2000), 105–109.
[4] N. Bakhvalov and G. Panasenko, *Averaging Processes in Periodic Media*, Nauka, Moscow, 1984.
[5] M.P. Bendsøe, *Optimization of Structural Topology, Shape, and Material*, Springer, 1995.
[6] A. Bensoussan, J.L. Lions and G. Papanicolaou, *Asymptotic Analysis for Periodic Structures*, North-Holland, Elsevier Science Publishers, Amsterdam, 1978.
[7] V.V. Jikov, S.M. Kozlov and O.A. Oleinik, *Homogenization of Differential Operators and Integral Functionals*, Springer, 1994.
[8] K. Suzuki and N. Kikuchi, A homogenization method for shape and topology optimization, *Comput. Meth. Appl. Mech. Engrg.* **93** (1991), 291–318.
[9] R.H.W. Hoppe and S.I. Petrova, Structural optimization of biomorphic microcellular ceramics by homogenization approach, *Lect. Notes Comput. Sci., Springer* **2179** (2001), 353–360.
[10] R.H.W. Hoppe and S.I. Petrova, *Homogenized elasticity solvers for biomorphic microcellular ceramics*, Proc. ENUMATH 2001, July 23–28, 2001, Ischia, Italy, F. Brezzi ed., Springer, 2003, pp. 371–380.
[11] R.H.W. Hoppe, S.I. Petrova and V. Schulz, Primal-dual Newton-type interior-point method for topology optimization, *J. Optim. Theory Appl.* **114** (2002), 545–571.
[12] G. Wittum, On the convergence of multigrid methods with transforming smoothers. Theory with applications to the Navier-Stokes equations, *Numer. Math.* **57** (1989), 15–38.
[13] H.A. Van der Vorst, Bi-CGSTAB: A fast and smoothly converging variant of Bi-CG for the solution of nonsymmetric linear systems, *SIAM J. Sci. Stat. Comput.* **13** (1992), 631–644.
[14] D.M. Gay, M.L. Overton and M.H. Wright, *A Primal-Dual Interior Method for Nonconvex Nonlinear Programming*, Advances in Nonlinear Programming, Y. Yuan, ed., Kluwer, Dordrecht, Holland, 1998, pp. 31–56.